The Journal of Neuroscience, August 1, 1997, 17(15):5868–5880

Cortistatin Is Expressed in a Distinct Subset of Cortical Interneurons

Luis de Lecea,[1] José Antonio del Rio,[3] José R. Criado,[2] Soledad Alcántara,[3] Marisela Morales,[2] Patria E. Danielson,[1] Steven J. Henriksen,[2] Eduardo Soriano,[3] and J. Gregor Sutcliffe[1]

Departments of [1]Molecular Biology and [2]Neuropharmacology, The Scripps Research Institute, La Jolla, California 92037, and [3]Unitat de Biologia Cel.lular, Facultat de Biologia, Universitat de Barcelona, Barcelona, 08028 Spain

Cortistatin is a presumptive neuropeptide that shares 11 of its 14 amino acids with somatostatin. In contrast to somatostatin, administration of cortistatin into the rat brain ventricles specifically enhances slow wave sleep, apparently by antagonizing the effects of acetylcholine on cortical excitability. Here we show that preprocortistatin mRNA is expressed in a subset of GABAergic cells in the cortex and hippocampus that partially overlap with those containing somatostatin. A significant percentage of cortistatin-positive neurons is also positive for parvalbumin. In contrast, no colocalization was found between cortistatin and calretinin, cholecystokinin, or vasoactive intestinal peptide. During development there is a transient increase in cortistatin-expressing cells in the second postnatal week in all cortical areas and in the dentate gyrus. A transient expression of preprocortistatin mRNA in the hilar region at P16 is paralleled by electrophysiological changes in dentate granule cells. Together, these observations suggest mechanisms by which cortistatin may regulate cortical activity.

Key words: cortistatin; preprocortistatin; mRNA; slow wave sleep; GABAergic stimulation; somatostatin

We recently isolated a cDNA clone of the rat mRNA encoding preprocortistatin, the putative 112 amino acid precursor of a novel neuropeptide structurally related to somatostatin (de Lecea et al., 1996). Cortistatin shares 11 of 14 residues with somatostatin, including those that are known to be responsible for somatostatin binding to its receptors (Veber et al., 1979) and the cysteines that are likely to render the peptide cyclic. The cDNA sequence and chromosomal localization of cortistatin and somatostatin indicate clearly that they are the products of separate genes (de Lecea et al., 1996, 1997). Synthetic cortistatin was shown to share several biological properties with somatostatin (de Lecea et al., 1996), but its effects on cortical electrical activity and sleep were distinct from those found for somatostatin. Moreover, cortistatin was shown to antagonize the effects of acetylcholine on cortical measures of excitability, whereas somatostatin enhances acetylcholine release and potentiates acetylcholine responses (Mancillas et al., 1986; Araujo et al., 1990). These observations demonstrated that cortistatin is functionally distinct from somatostatin and raised the possibility that cortistatin exerts its activities via an uncharacterized cortistatin-selective receptor, although other explanations of different functionalities can be considered.

Preliminary *in situ* hybridization studies to determine the anatomical locations of the cells that produce preprocortistatin detected scattered cells throughout the cortex and hippocampus. The positions of these cells in relation to pyramidal cells of the hippocampus suggested that they were inhibitory interneurons, a hypothesis consistent with the electrophysiological findings (de Lecea et al., 1996). The complex population of intrinsic inhibitory GABAergic neurons in the cortex and hippocampus has been subgrouped by its specific afferent connectivity and the presence of calcium-binding proteins (calbindin, parvalbumin, and calretinin; de Felipe, 1993; Cauli et al., 1997; Kondo et al., 1997) and neuropeptides [cholecystokinin (CCK), Hendry and Jones (1985); vasoactive intestinal peptide (VIP), Morrison et al. (1984); neuropeptide Y (NPY) and somatostatin (SST), Hendry et al. (1984a), Schmechel et al. (1984), Somogyi et al. (1984), and Freund and Buzsáki (1996)]. Calbindin-containing cortical interneurons are also positive for several neuropeptides and are known to make somatodendritic contacts with pyramidal cells (Gulyás and Freund, 1996). On the other hand, parvalbumin is expressed in a nonoverlapping set of fast-firing interneurons that make GABAergic synapses on cell bodies and axon initial segments of projection cells (Celio, 1986; Kawaguchi and Hama, 1987; de Lecea et al., 1995). The distribution of calretinin partially overlaps with calbindin and labels additional GABAergic cells (Jacobowitz and Winsky, 1991; Miettinen et al., 1992; Acsády et al., 1993).

Here we show that the cortistatin-expressing cells of the cortex and hippocampus are GABAergic and positive for calbindin and parvalbumin. We examine the relationships between somatostatin- and cortistatin-containing cells and find that in many areas they are independent populations, but in some regions there are variable extents of coexpression. We also analyze the appearance of cortistatin mRNA in the cerebral cortex and hippocampus during development and use electrophysiological techniques *in vivo* to correlate functional changes with the transient expression of cortistatin in the dentate gyrus. These results, together with previous physiological observations, suggest mechanisms by which cortistatin may regulate cortical activity.

MATERIALS AND METHODS

In situ *hybridization.* We conducted *in situ* hybridization essentially as described elsewhere (de Lecea et al., 1994) with minor modifications.

Received March 24, 1997; revised May 19, 1997; accepted May 20, 1997.

This work was supported in part by grants from the National Institute of General Medical Sciences and Comisión Interministerial de Ciencia y Tecnología, Spain. We thank Allan Tobin for providing the rat GAD65 and GAD67 plasmids.

Correspondence should be addressed to Dr. J. Gregor Sutcliffe at the above address.

Briefly, Sprague Dawley rats at various developmental stages (P0, P5, P10, P12, P16, P21, and adults) were anesthetized and perfused intracardially with 4% paraformaldehyde (PF) in PBS, pH 7.4. Brains were removed and post-fixed in the same fixative overnight and cryoprotected in sucrose dissolved in 4% PF. Then brains were frozen, and sections 25 μm thick were collected in cryoprotectant solution (30% glycerol, 30% ethylene glycol, and 0.1 M PBS). Free-floating sections were incubated in 0.1% Triton X-100 in PBS, deproteinized with 0.1N HCl for 10 min, acetylated with acetic anhydride (0.25% in 0.1 M triethanolamine hydrochloride, pH 8), post-fixed for 10 min in 4% PF, and prehybridized at 55°C for 3 hr in a solution containing 6× PIPES, 10% (w/v) dextran sulfate, 50% formamide, 5× Denhardt's, 40 mM DTT, 100 μg/ml yeast RNA, and 100 μg/ml denatured salmon sperm DNA. We labeled a cortistatin riboprobe by *in vitro* transcription of a 128 bp fragment (nucleotides 310–438) encoding rat cortistatin, using T3 polymerase (Ambion, Austin, TX) and ^{35}S-uridine 5′-triphosphate (UTP) (DuPont NEN, Boston, MA). Labeled antisense cRNA was added to the sections (10^7 cpm/ml) and incubated overnight at 55°C. Sections were transferred to new vials and washed with 2× SSC, 10 mM β-mercaptoethanol (β-ME) (room temperature for 10 min), digested with RNase A (37°C for 1 hr), and washed again with 1× SSC, 50% formamide, 5 mM β-ME (55°C for 1 hr), and 0.1× SSC plus 0.1% Sarkosyl (30 min, 68°C). Sections were mounted on coated slides (Fisher Scientific, Houston, TX) and exposed to x-ray film and later to Ilford K5 autoradiographic emulsion for 4 weeks at 4°C. We developed the slides with Kodak D19 and counterstained with Richardson's blue. A sense cRNA probe, transcribed with T7 RNA polymerase, was included as a negative control for most hybridization experiments.

Double-label in situ *hybridization.* We labeled the two isoforms of rat glutamic acid decarboxylase (GAD 65 and GAD 67, generously provided by Dr. Allan Tobin, University of California Los Angeles, Los Angeles, CA) with digoxigenin (DIG; Boehringer Mannheim, Indianapolis, IN) and T3 RNA polymerase by *in vitro* transcription, as described by the manufacturer. We pretreated the tissue as described above and added 10^7 cpm/ml ^{35}S-labeled cortistatin and 200 ng of DIG-labeled GAD65 or GAD67. After being washed at high stringency, sections were incubated with an alkaline phosphatase-conjugated antibody to DIG (1:5000; Boehringer Mannheim) and developed with nitroblue tetrazolium and 5-bromo-4-chloro-3-indolyl phosphate (BCIP) alkaline phosphatase substrates (Life Technologies, Gaithersburg, MD). We then mounted the sections and dipped them in emulsion, as described above.

Combined immunohistochemistry with in situ *hybridization.* To detect both protein and mRNA in the same sections, we conducted *in situ* hybridization first and then incubated the sections with primary antibodies for 12 hr at 4°C, as described (Alcántara et al., 1996). After washing the sections with PBS, we incubated with biotinylated secondary antibodies and ABC–peroxidase (Vector Laboratories, Burlingame, CA). We used 0.5 mg/ml diaminobenzidine (filtered through 0.22 μm; Sigma, St. Louis, MO) and 0.01% H_2O_2 as peroxidase substrates. Then sections were mounted and dipped in emulsion. Calbindin-specific (1:2000), calretinin-specific (1:2000), and parvalbumin-specific (1:3000) antibodies were obtained from SWant (Bellinzona, Switzerland). Antisera to VIP (1:500), CCK (1:1000), or somatostatin (1:2000) have been characterized elsewhere (Morrison et al., 1983). The antibody to somatostatin (S328) recognizes the N-terminal region of somatostatin-28 and therefore is unlikely to cross-react with cortistatin.

Data analysis. Sections were examined with a Zeiss Axiophot microscope (Oberkochen, Germany). The delimitation of regional and laminar boundaries was performed according to Zilles (1985). For the quantitative analysis of labeled neurons, only sections processed in parallel under exactly the same conditions and displaying similar background levels (<10 grains/100 μm^2) were considered. Because the autoradiographic background levels were less than six grains per cell, neuronal somata were considered positive when overlaid by 15 or more silver grains, although positive neurons normally displayed >25 grains. Sections hybridized with a sense riboprobe never exceeded the background threshold. Two different animals were analyzed for each age. To determine the radial distribution of cortistatin mRNA-positive cells, we harvested eight vertical strips (250 μm wide) covering the entire cortical thickness in the following areas: somatosensory (first parietal area, PAR1), motor (hindlimb–forelimb, HL–FL), and visual (primary monobinocular, occipital, OC1M-B) cortices and hippocampal CA1. The number of labeled cells in single layers was counted and their percentage relative to the remaining cortical laminae calculated. For quantitative analysis of double-labeled neurons, the numbers of immunoreactive cells displaying positive and negative hybridization in the somatosensory cortex were counted in 6–15 sections from two to three animals for each neurochemical marker. Densities of cortistatin-expressing cells were determined by counting positive cells in eight frames (650 × 440 μm) corresponding to the somatosensory and visual areas of three different animals.

Northern blot. Cytoplasmic RNA from whole brain samples of Sprague Dawley rats at various developmental stages (except E14, in which the whole head was homogenized) was extracted as described (Schibler et al., 1980). Two micrograms of poly(A^+) RNA were run on agarose formaldehyde gels, transferred to nylon membranes, and hybridized with a ^{32}P-labeled cortistatin probe. Cyclophilin was used as a control probe for loading and RNA integrity (Danielson et al., 1988).

Electrophysiology. Male Sprague Dawley rats (adult group: 280–300 gm, 50–60 d old; P15 group: 27–31 gm, 15–17 d old) were anesthetized with halothane (3–4%) and placed into a stereotaxic apparatus. Halothane was adjusted to 0.7–0.9% on completion of surgery and maintained at that level throughout the duration of the experiment. Body temperature was measured and maintained at 37°C ± 0.5°C by a feedback-regulated heating pad. Evoked field potentials were recorded by one-barrel micropipette (3.0 M NaCl filled; 6–11 mΩ; 1–2 μm, i.d.) glued to a four-barrel iontophoresis electrode (tip extending 10 μm ahead of the multibarrel tip) stereotaxically oriented into the dentate gyrus (coordinates: 2.5–3.5 mm posterior and 2.0–2.5 mm lateral to bregma; 2.4–3.0 mm ventral from dura). Acquisition, analysis, and processing of data on- and off-line were performed by customized National Instruments LabVIEW software on Macintosh computers. Square-wave constant pulses (0.2–1.4 mA; 0.15 msec duration) were generated by a Grass PSIU6 isolation unit controlled by a MASTER 8 pulse generator. Population spikes (PS) were elicited in the dentate gyrus by stimulation of the angular bundle of the perforant path (coordinates: 6.0–8.1 mm posterior and 4.0–4.2 mm lateral from bregma; 2.5–3.5 mm ventral from dura) with insulated, bipolar stainless steel electrodes. Paired-pulse curves were tested by administering two stimuli with varying interstimulus intervals (10–260 msec) at half-maximum stimulus intensity. The PS amplitude evoked by the second stimulus was expressed as a percentage of the first. Cortistatin (1 mg/ml) was dissolved in saline and administered iontophoretically through one barrel of a multibarreled micropipette with Medical Systems (Greenvale, NY) IP-2 iontophoresis pumps and BH-2 balance unit. We routinely used retention (backing) currents of 5–15 nA and automated balance in the side NaCl barrel to reduce polarization artifacts. Cortistatin was ejected by positive currents (50–150 nA) and retained with negative currents. Results of experimental groups from calculations performed on the stimulus–response and paired-pulse data were expressed as mean ± SEM. Results were compared by repeated measures or completely randomized design ANOVA.

RESULTS

Distribution of cortistatin-positive cells

We used *in situ* hybridization to analyze the expression of preprocortistatin mRNA in adult rat brain. Film autoradiography of coronal sections showed a discrete and punctate pattern throughout the cerebral cortex and hippocampus, possibly corresponding to single neurons. Weak hybridization labeling was observed in the striatum and olfactory bulb, but no signals could be detected in the thalamus, midbrain, cerebellum, or spinal cord. Of note, signals were also absent from hypothalamus, an important site of somatostatin expression.

We examined the sections by emulsion autoradiography. The cerebral cortex was the area of the brain that contained the most cortistatin-positive cells. In the neocortex cortistatin mRNA-expressing neurons were found in all cortical areas and layers, except in layer I (Fig. 1*A,B*). In all cortical regions cortistatin-positive neurons were most abundant in layers II–III and VI (Fig. 2). There were also clear differences in the number of positive cells and intensity of hybridization in different cortical areas. The visual/temporal cortex displayed approximately twice as many cortistatin-positive cells as other areas, especially in the upper layers (294 ± 8 cells/mm^2 in visual cortex; 162 ± 6 cells/mm^2 in somatosensory cortex; Figs. 1*A–C*, 2).

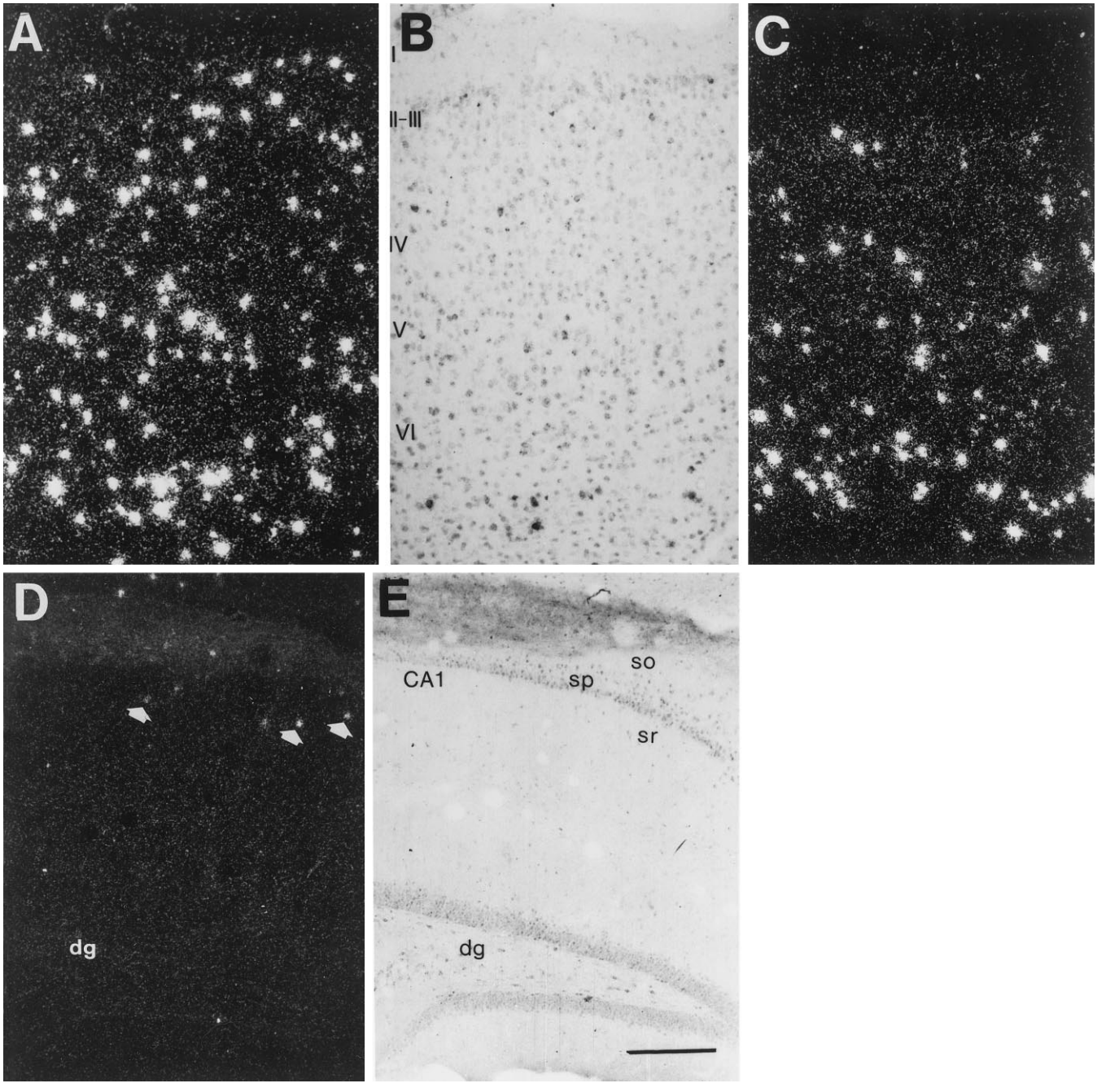

Figure 1. Cortistatin expression in the adult cortex. *A*, Dark-field view of a coronal section of the rat visual cortex hybridized with a cortistatin riboprobe. Very heavy labeling was observed in the deep layers, whereas in the upper layers both the number of positive cells and their cortistatin mRNA concentration were lower. *B*, The bright-field image of *A*. *C*, *In situ* hybridization of preprocortistatin mRNA in the somatosensory cortex. Note that there are substantially fewer cells in the upper layers, as compared with *A*. *D*, Dark-field micrograph of a coronal section across the hippocampal formation, which includes the granule cell layer of the dentate gyrus. Some labeling was found in the *CA1* field (*arrows*), especially in the stratum oriens (*so*), although some neurons in the pyramidal cell layer (*sp*) and stratum radiatum (*sr*) also could be detected. Very few or no labeled cells were found in the dentate gyrus (*dg*). *E*, Bright-field view of *D*. Scale bar, 100 μm.

Cortistatin-positive neurons were present in layer III of the piriform cortex as well as in layers III–IV of the entorhinal area. In the hippocampal region cortistatin mRNA-expressing neurons were scattered through the subiculum and CA1 region, where they were concentrated in the stratum oriens and to a lesser extent in the pyramidal layer (Fig. 1*D,E*). Cortistatin-positive cells were present in the CA3 region at low density (fewer than five cells per section). In the adult, hybridization signals were virtually absent from the hilus, but a few neurons (two to three cells per section) could be detected in the granule cell layer (Fig. 1*D,E*).

Other areas of the brain also showed cortistatin hybridization, although at lower intensity. In the olfactory bulb, granule GABAergic neurons were heavily labeled with autoradiographic silver grains. In the striatum a small number of positive cells resembling cholinergic or GABAergic interneurons displayed very low levels of hybridization. A few cells in the periventricular

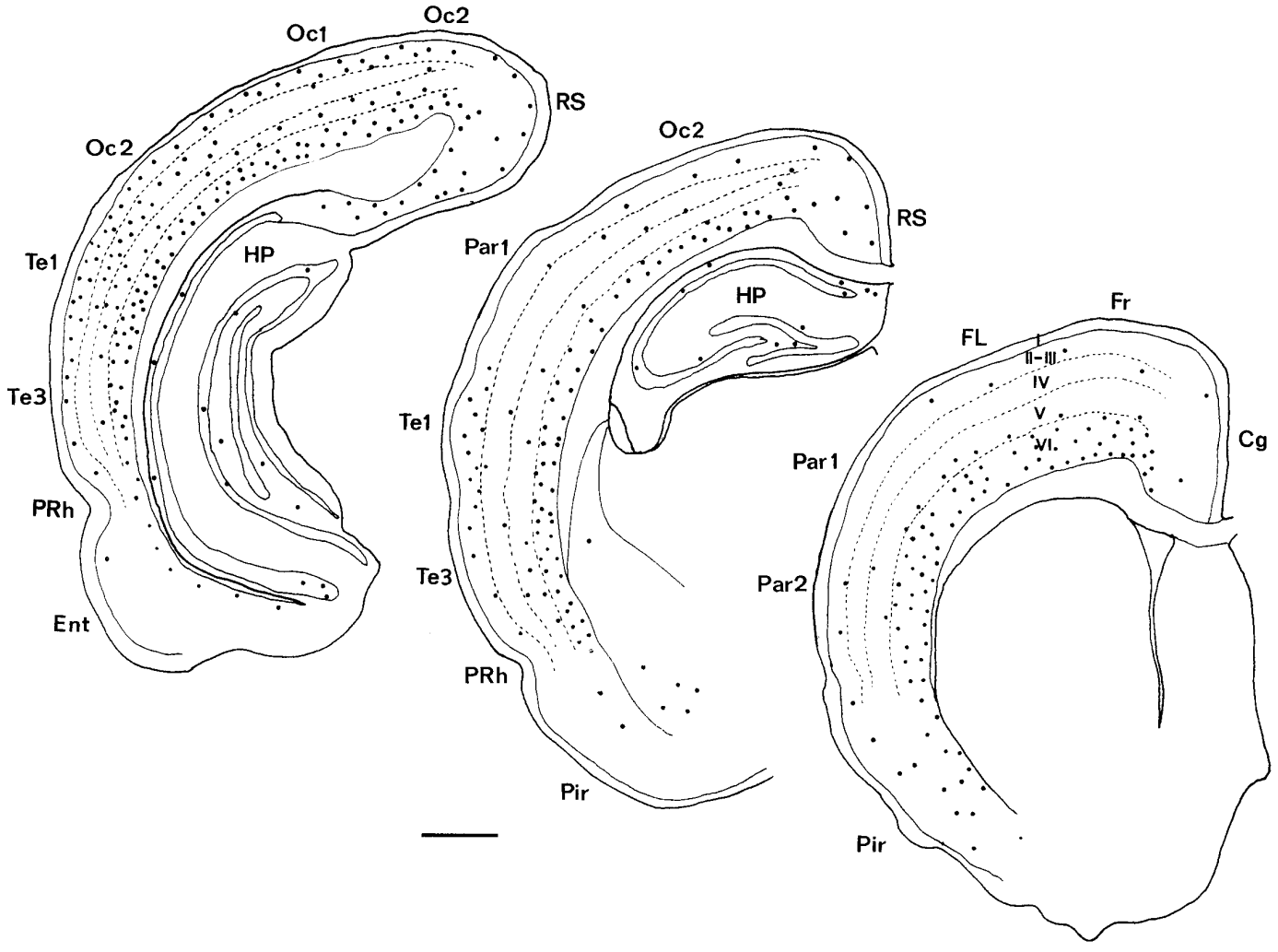

Figure 2. Camera lucida drawings showing the distribution of cortistatin mRNA in coronal sections of the cerebral cortex of adult rats at three different rostrocaudal levels. Each *dot* represents three labeled cells. *Cg*, Cingulate cortex; *Ent*, entorhinal cortex; *Fr*, frontal cortex; *FL*, forelimb area; *HP*, hippocampus; *Oc1*, occipital cortex, area 1; *Oc2*, occipital cortex, area 2; *Par1*, parietal cortex, area 1; *Par2*, parietal cortex, area 2; *Pir*, piriform cortex; *PRh*, perirhinal cortex; *RS*, retrosplenial cortex; *Te1*, temporal cortex, area 1; *Te3*, temporal cortex, area 3; *I–VI*, cortical layers. Scale bar, 1 mm.

hypothalamic nucleus, which were detected only with very long exposures of emulsion autoradiography, were positive for cortistatin mRNA. No signals were detected in the thalamus, mesencephalon, brainstem, cerebellum, or spinal cord.

Cortistatin is expressed exclusively in GABAergic interneurons

The above pattern of localization suggested that cortistatin mRNA might be present in a subset of GABAergic nonpyramidal interneurons. To confirm the GABAergic nature of cortistatin-expressing cells, we used double *in situ* hybridization for cortistatin and GAD65/GAD67 mRNAs. We labeled a rat cortistatin riboprobe with ^{35}S-UTP and the rat GAD65 and GAD67 probes with DIG. In both the neocortex and hippocampus (Fig. 3*A*) all cortistatin-positive cells were also positive for GAD65 or GAD67. More cortistatin-labeled cells were positive for GAD65 (77%) than for GAD67 (40%) in all cortical layers, probably reflecting the ratio of GAD65/67 expression in the neocortex. These results suggest that most, if not all, cortistatin-positive cells are GABAergic.

Cortistatin and somatostatin label different populations of interneurons

Somatostatin also is expressed by GABAergic interneurons (Kosaka et al., 1988; Esclápez and Houser, 1995). To compare the distributions of cortistatin and somatostatin, we combined immunocytochemical staining for somatostatin with *in situ* hybridization for preprocortistatin. Strikingly, the two statins exhibited similar radial patterns of distribution being concentrated in layers II–III and VI. However, fewer than one-half of the cortistatin-positive neurons (42%, visual cortex; 33%, somatosensory cortex) displayed somatostatin immunoreactivity. Conversely, one-fourth (23% in somatosensory cortex; 28% in visual cortex) of somatostatin-immunoreactive neurons displayed cortistatin hybridization signals, demonstrating that cortistatin and somatostatin are expressed in different populations of neurons (Figs. 3*B*, 4*A*). There were also notable differences in the degree of colocalization among the cortical layers. For instance, in layer II–III and IV most positive neurons expressed either somatostatin or cortistatin but not both, whereas in deep cortical layers (especially

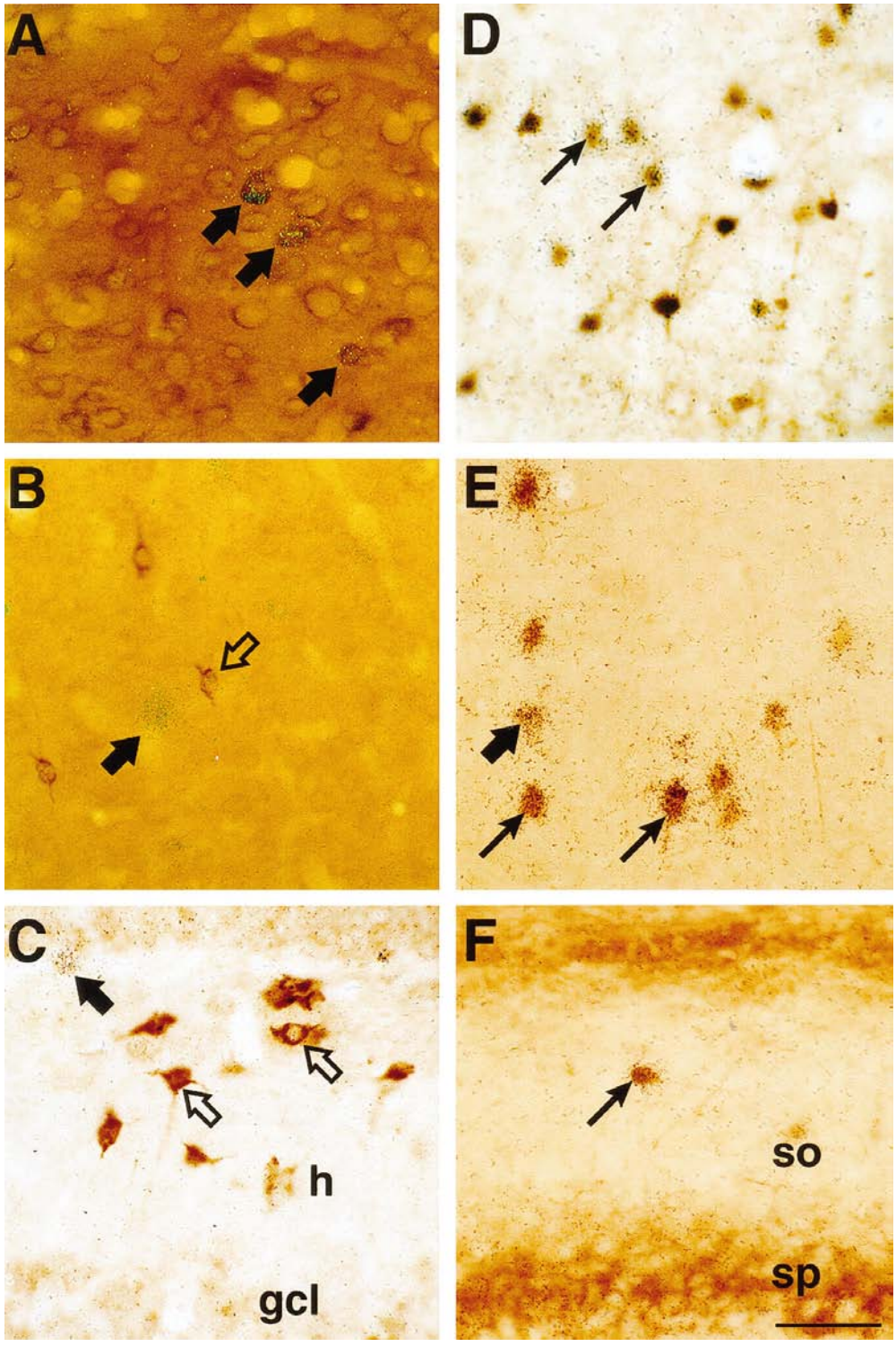

Figure 3. Colocalization of preprocortistatin mRNA with different markers of cortical interneurons. *A*, Cortistatin-positive cells (clusters of silver grains) overlap with digoxigenin-labeled GAD65-positive cells (*arrows*). *B*, In the upper layers of the neocortex, cortistatin-positive cells (*filled arrow*) do not overlap with somatostatin-immunoreactive cells (*open arrow*). *C*, The dentate gyrus, which is abundant in somatostatin immunoreactivity (*open arrows*), contains very few cortistatin-expressing cells that are localized in the granule cell layer (*filled arrow*); *h*, hilar region; *gcl*, granule cell layer. *D*, A significant number of cortistatin-positive cells was also positive for parvalbumin immunoreactivity in the visual cortex (double-positive cells are marked by *thin arrows*). *E*, Cortistatin mRNA frequently colocalized with calbindin-immunoreactive material, especially in the deep layers of the visual neocortex (double-positive cells are marked by *thin arrows*). A cortistatin-only positive cell is marked with a *thick arrow*. *F*, In the hippocampus cortistatin mRNA was present in a subset of parvalbumin-positive interneurons (*thin arrow*); *so*, stratum oriens; *sp*, stratum pyramidale. Scale bar, 50 μm.

in layer VI) as many as 44% of cortistatin-positive cells also contained somatostatin-like immunoreactivity (Fig. 4).

In the hippocampal CA1 field 58% of cortistatin-positive cells were also immunoreactive for somatostatin. However, cortistatin/somatostatin-positive cells represented ~30% of the somatostatin population (Fig. 4*B*). The subiculum displayed a complex mixture of labeled populations. In contrast, only very rarely could we detect the presence of cortistatin mRNA in the hilar region of adult animals, which was rich in somatostatin-positive cells (Fig. 3*C*). These findings show that cortistatin and somatostatin are expressed in different, although partially overlapping, populations of cortical interneurons.

Cellular characterization of cortistatin neurons

To characterize further the types of cortical interneurons that expressed cortistatin, we used combined *in situ* hybridization for preprocortistatin mRNA with immunocytochemistry to the calcium-binding proteins parvalbumin, calbindin, and calretinin

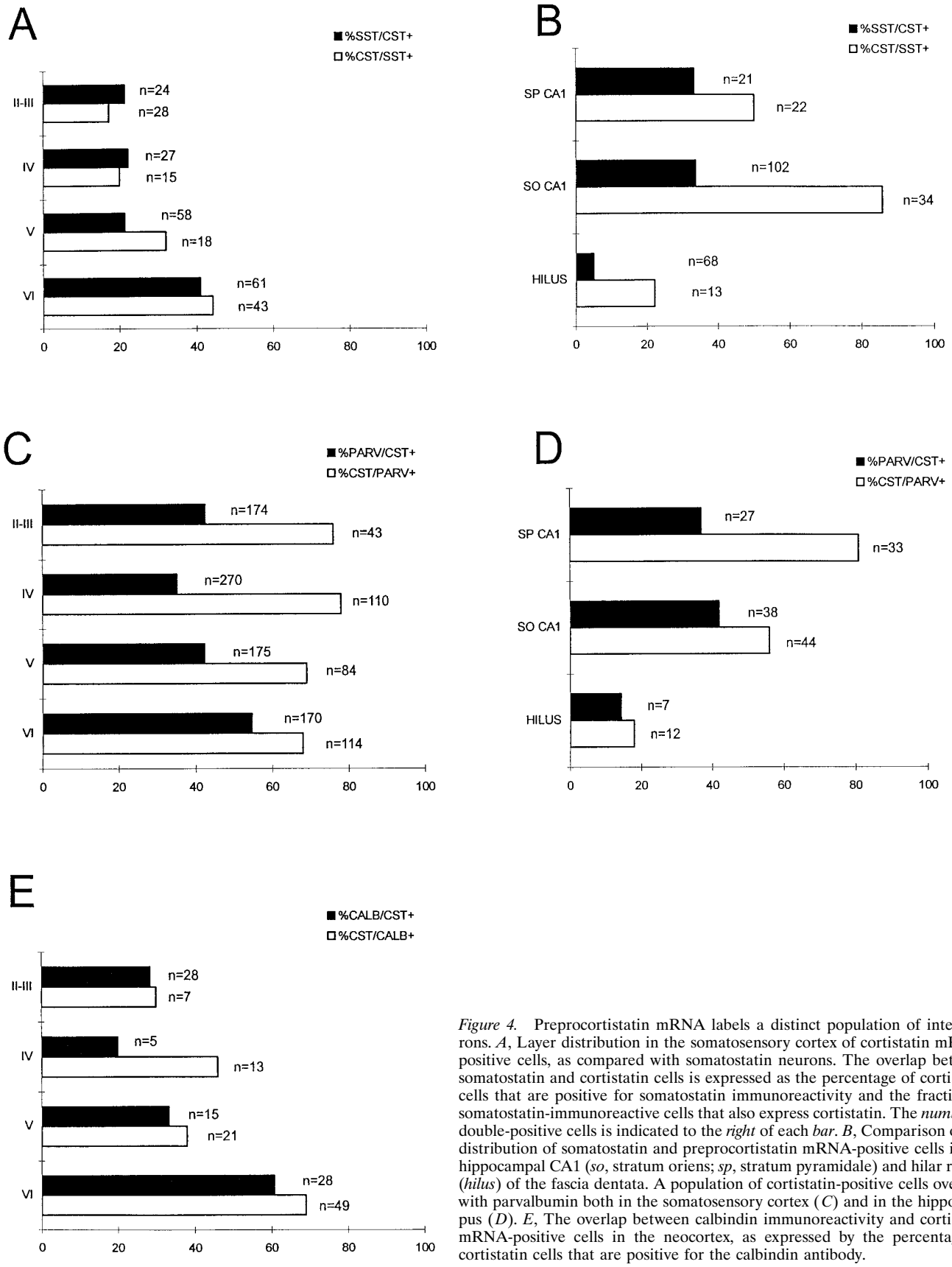

Figure 4. Preprocortistatin mRNA labels a distinct population of interneurons. *A*, Layer distribution in the somatosensory cortex of cortistatin mRNA-positive cells, as compared with somatostatin neurons. The overlap between somatostatin and cortistatin cells is expressed as the percentage of cortistatin cells that are positive for somatostatin immunoreactivity and the fraction of somatostatin-immunoreactive cells that also express cortistatin. The *number* of double-positive cells is indicated to the *right* of each *bar*. *B*, Comparison of the distribution of somatostatin and preprocortistatin mRNA-positive cells in the hippocampal CA1 (*so*, stratum oriens; *sp*, stratum pyramidale) and hilar region (*hilus*) of the fascia dentata. A population of cortistatin-positive cells overlaps with parvalbumin both in the somatosensory cortex (*C*) and in the hippocampus (*D*). *E*, The overlap between calbindin immunoreactivity and cortistatin mRNA-positive cells in the neocortex, as expressed by the percentage of cortistatin cells that are positive for the calbindin antibody.

and to two neuropeptides. Together, these proteins are known to define several subpopulations of cortical interneurons (Freund and Buzsáki, 1996). Cortistatin mRNA colocalized frequently with parvalbumin, especially in layers II–III of the visual and somatosensory cortices (73%; Fig. 3*D*) and in the pyramidal layer of the CA1 hippocampal field (75%; Fig. 3*F*). Double-labeled cortistatin/parvalbumin-positive neurons represented ~40% of the entire population of parvalbumin-immunoreactive neurons (Fig. 4*C,D*).

In the deep layers of the cortex 47% of cortistatin mRNA-expressing neurons were labeled with calbindin antibodies, whereas in the supragranular layers and in the hippocampus colocalization was rare. The double-labeled slides immunoreacted for calbindin, which labels faintly most pyramidal and granule cells in cortical layers II–III and IV and in the hippocampus, also confirmed that these principal neurons did not express cortistatin mRNA (Fig. 3*E*). We rarely detected double-labeled neurons immunoreactive for calretinin. Finally, cortical interneurons immunoreactive for CCK or VIP did not express cortistatin mRNA (data not shown). These findings show that cortistatin is expressed in a subset of calbindin- and parvalbumin-positive interneurons.

Developmental pattern of preprocortistatin mRNA accumulation

We examined the pattern of accumulation of cortistatin mRNA during development. By Northern blot a single 600 nucleotide band, corresponding to preprocortistatin mRNA, accumulated postnatally between P5 and P10, achieved its maximal levels by P15, and then decayed slightly into adulthood (Fig. 5). *In situ* hybridization showed cortistatin-positive cells in the lower levels of the cerebral cortex and the stratum oriens of the hippocampus as early as P0, the earliest time point analyzed (Figs. 5–7). Stronger hybridization signals could be detected at this stage in the cingulate cortex and in the induseum griseum, taenia tecta, and subiculum (Fig. 6*A,B*). At P5 both the number of cortistatin mRNA-expressing cells and the individual intensity of labeling were increased in the neocortex, although the distribution of labeled cells remained the same, with most positive neurons being concentrated in infragranular layers. A conspicuous increase in cortistatin expression was noted in the hippocampus, which now showed many intensely labeled neurons in both the stratum oriens and pyramidal layer (Fig. 7).

At P10–P12 the levels of autoradiographic labeling increased further both in the neocortex and hippocampus (Figs. 5*B,C*, 7). Of note, some cortical areas such as the temporal and parietal cortices exhibited at these stages strong labeling in supragranular layers II–III and IV in addition to a large number of labeled neurons in the infragranular layers. In the P10–P12 hippocampus the distribution of cortistatin-positive cells was similar to that at P5, but at this later age approximately five to six positive cells per section could be detected in the hilar region. Hippocampal cortistatin-positive cells showed intense hybridization signals at these ages.

At P16–P21 there was a much stronger labeling than at P12, as judged both by the density of silver grains per cell and by the number of positive cells in all cortical areas (Figs. 6–7). In the neocortex a nearly uniform pattern of expression was observed, with all cortical areas displaying a large number of positive neurons in both the deep cortical layers and the supragranular layers. Also, the number of cortistatin-positive cells in all cortical areas was greater than in the adult (480 ± 23 cells/mm^2 in P16 vs 263 ± 15 cells/mm^2 in adult rats; Fig. 6*E*). In the hippocampus there were more labeled cells at P16 than in both earlier and adult stages (68 ± 7 cells/section at P16, as compared with 51 ± 5.3 cells in the adult; Fig. 6*F*). This was particularly evident in the hilar region, where cortistatin-expressing cells were virtually absent in the adult.

Electrophysiological characterization of cortistatin actions on dentate function during development

Because the expression of cortistatin mRNA in the dentate hilar region was significantly higher at P15 than in the adult, we examined the effects of cortistatin on dentate function during these developmental stages. To investigate whether the adult disappearance of cortistatin mRNA in hilar interneurons could be paralleled by physiological and pharmacological changes in granule cells, we conducted electrophysiological studies *in vivo* to characterize the effects of local application of cortistatin on the excitability of granule cells and on the efficacy of local inhibitory circuits in the dentate gyrus. Stimulation of the perforant path evoked field potentials recorded in the granule cell layer or hilus of the dentate gyrus, the wave forms of which consisted of a relatively fast negative-going PS superimposed on the positive-going field EPSP/IPSP complex. Consistent with previous reports (Wilson, 1984; Bekenstein and Lothman, 1991), we observed that PS amplitudes at half-maximal stimulation were significantly lower in P15 than in adults ($p < 0.005$; Fig. 8*A*). Iontophoretic administration of cortistatin had no significant effect on PS amplitudes in the adult dentate gyrus ($p > 0.05$; Fig. 8*B*). This contrasts with our previous observation that cortistatin inhibits PS amplitudes in the adult CA1 (de Lecea et al., 1996). Moreover, cortistatin suppressed PS amplitudes in the dentate gyrus of P15 rats by at least 40% in three of five animals ($p < 0.05$; Fig. 8*A*).

Equipotent paired orthodromic stimulation of the perforant path in the adult dentate gyrus elicited a triphasic test/conditioning response curve (Fig. 8*C*). In contrast, the early inhibitory phase of the paired-pulse response in P15 rats was significantly longer (Fig. 8*C*). Statistical analyses showed that paired-pulse responses in adult and P15 rats were significantly different at 40, 60, and 80 msec ($p < 0.05$; Fig. 8*C*; representative recordings are shown in Fig. 8*D,E*). These data are consistent with previous reports by Liu et al. (1996), suggesting that GABAergic synapses dominate the synaptic physiology of most immature granule cells. Iontophoretic administration of cortistatin had no effect on the paired-pulse responses elicited on either group ($p > 0.05$; Fig. 8*C*).

DISCUSSION

We have used a combination of immunocytochemical and *in situ* hybridization techniques to identify the cell types that express the precursor of the neuropeptide cortistatin in adult and developing rat cortex and hippocampus. We have shown that the novel neuropeptide cortistatin is expressed in a subpopulation of cortical GABAergic interneurons that comprises subsets of calbindin- and parvalbumin-immunoreactive cortical neurons. Preprocortistatin mRNA and somatostatin are expressed in distinct but partially overlapping populations of neurons. However, because colchicine was not used in this study, somatostatin-immunoreactive cells could have been under-represented. The percentages and distribution of colocalization among preprocortistatin mRNA, calbindin, and somatostatin suggest that the cells that are double-positive for cortistatin and calbindin are also positive for somatostatin. Cortistatin has been shown to bind to at least some somatostatin receptors with an affinity similar to that

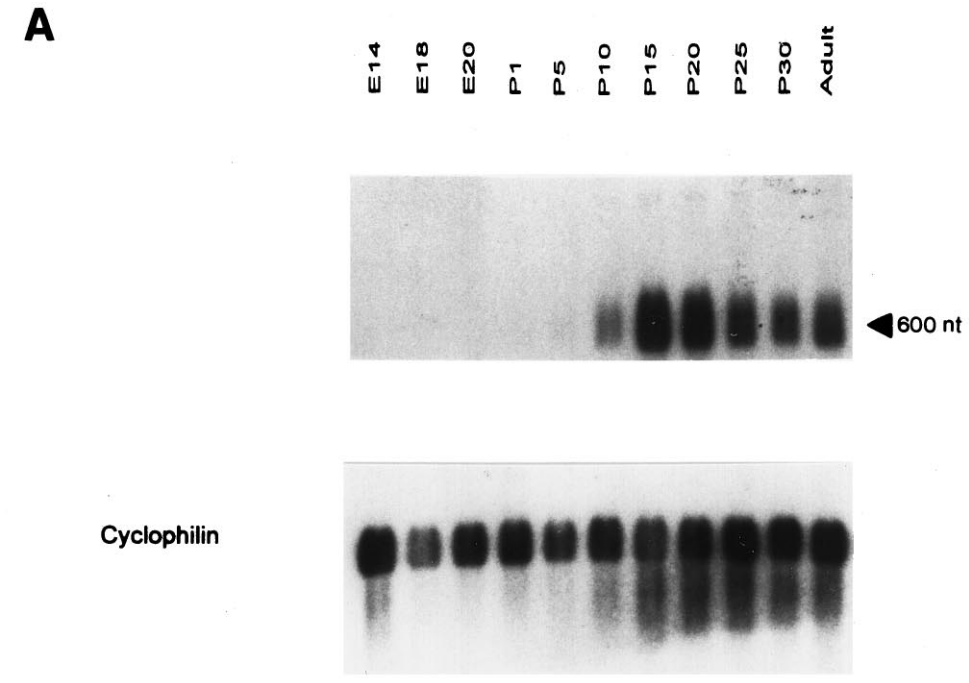

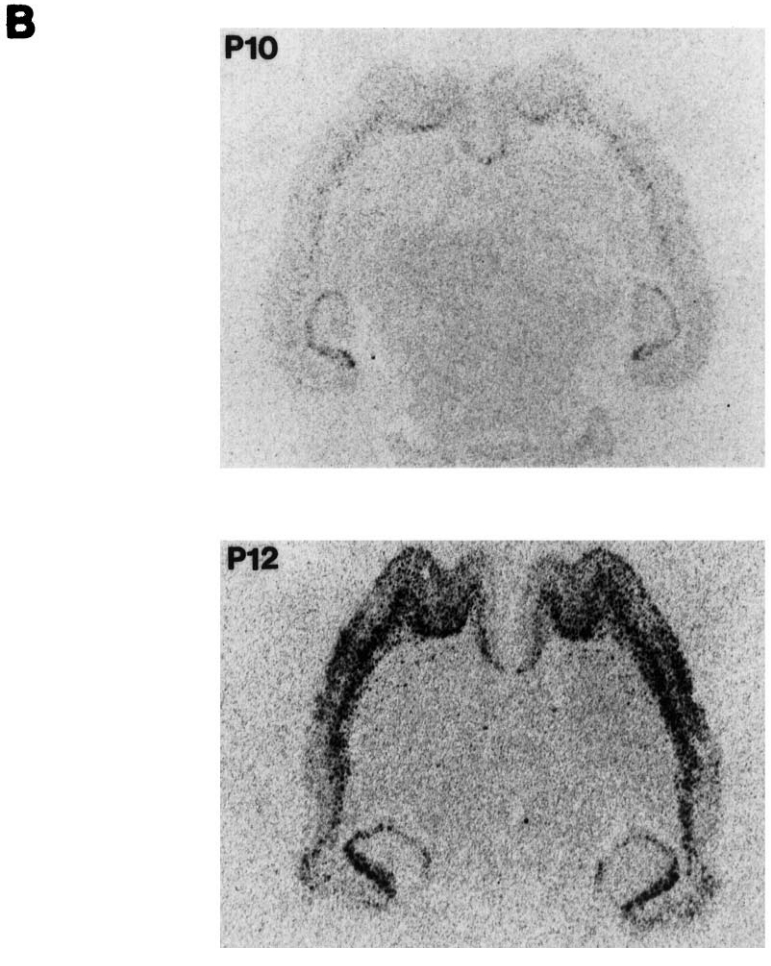

Figure 5. Preprocortistatin mRNA accumulation during development. *A*, Northern blot of mRNAs extracted from whole brain at different time points during rat development, hybridized with a cortistatin probe. The *E14* sample was obtained from whole head. An *arrow* indicates the length (as determined by interpolation with unshown markers) of the band that hybridized with the cortistatin cDNA probe, consistent with that reported for preprocortistatin mRNA (de Lecea et al., 1996, 1997). A cyclophilin probe was hybridized to the same blot as a control for RNA integrity and loading. *B*, Horizontal sections of an *in situ* hybridization to *P10* and *P12* rats showing that the increase in cortistatin signal is attributable to an increase in both the number of positive cells and in the concentration per cell.

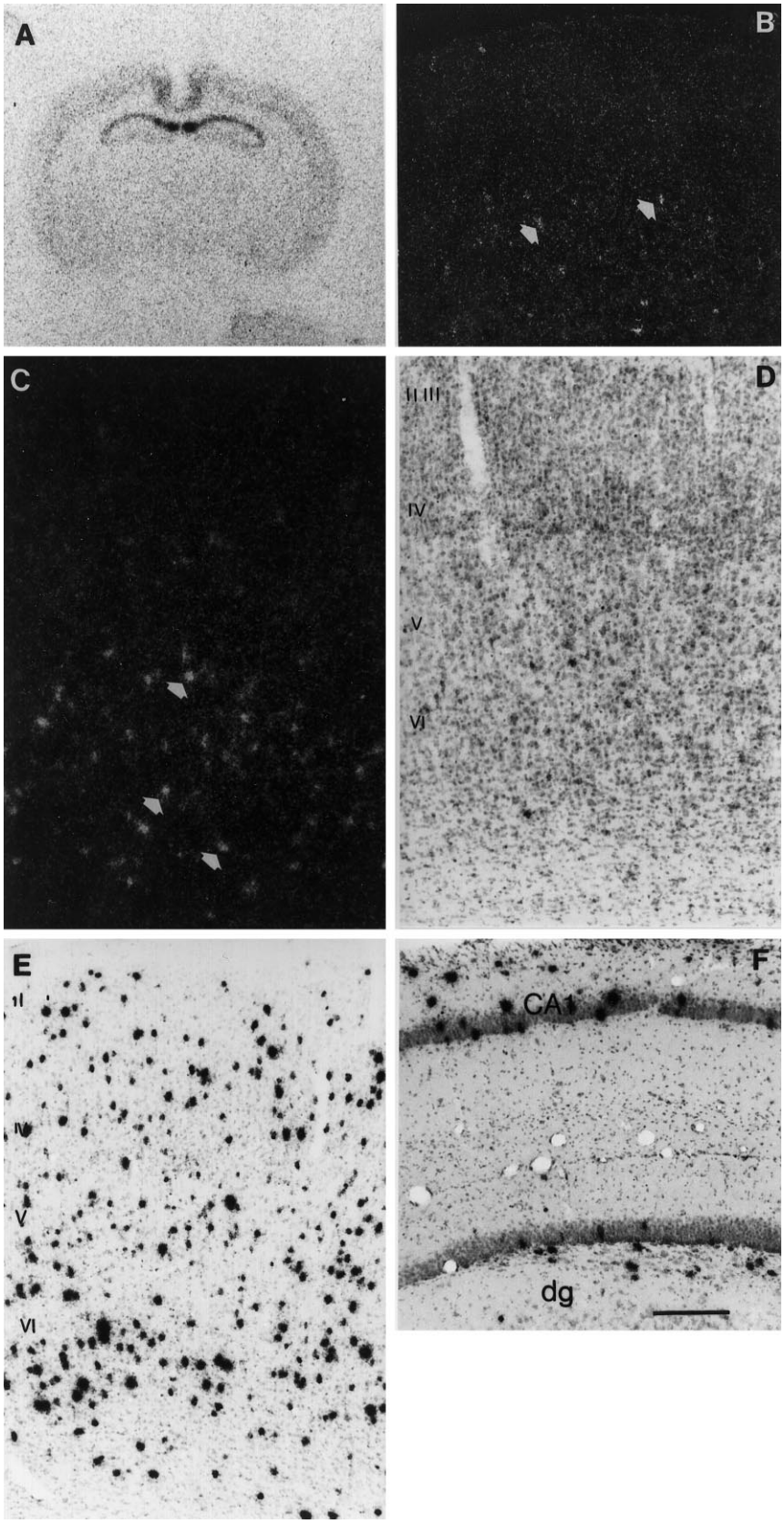

Figure 6. In situ hybridization of preprocortistatin mRNA in postnatal animals. *A*, Film autoradiograph of a coronal section of a P0 rat hybridized with a cortistatin riboprobe. Strong hybridization can be observed in the subiculum and CA1 region. *B*, Dark-field *in situ* hybridization of a coronal section of a P0 cortex. Very faint neurons were detected in the deep layers (*arrows*). Dark-field (*C*) and bright-field (*D*) micrographs of a P5 temporal cortex are shown. The hybridization levels were low to moderate and confined to the deep layers of the neocortex. *E*, Bright-field image of an *in situ* hybridization of a P16 parietal cortex. Note the very high levels of hybridization per cell, which are visible even at low power. The number of positive cells at this age was approximately three times that found in adult animals. *F*, Bright-field micrograph of a coronal section through the hippocampal formation of a P16 rat. Again, very high levels of hybridization could be detected in the *CA1* region, especially in the stratum oriens and pyramidale. Also, a substantial increase in the number of cells in the granule cell layer and hilar region was evident at this age. *dg*, Dentate gyrus.

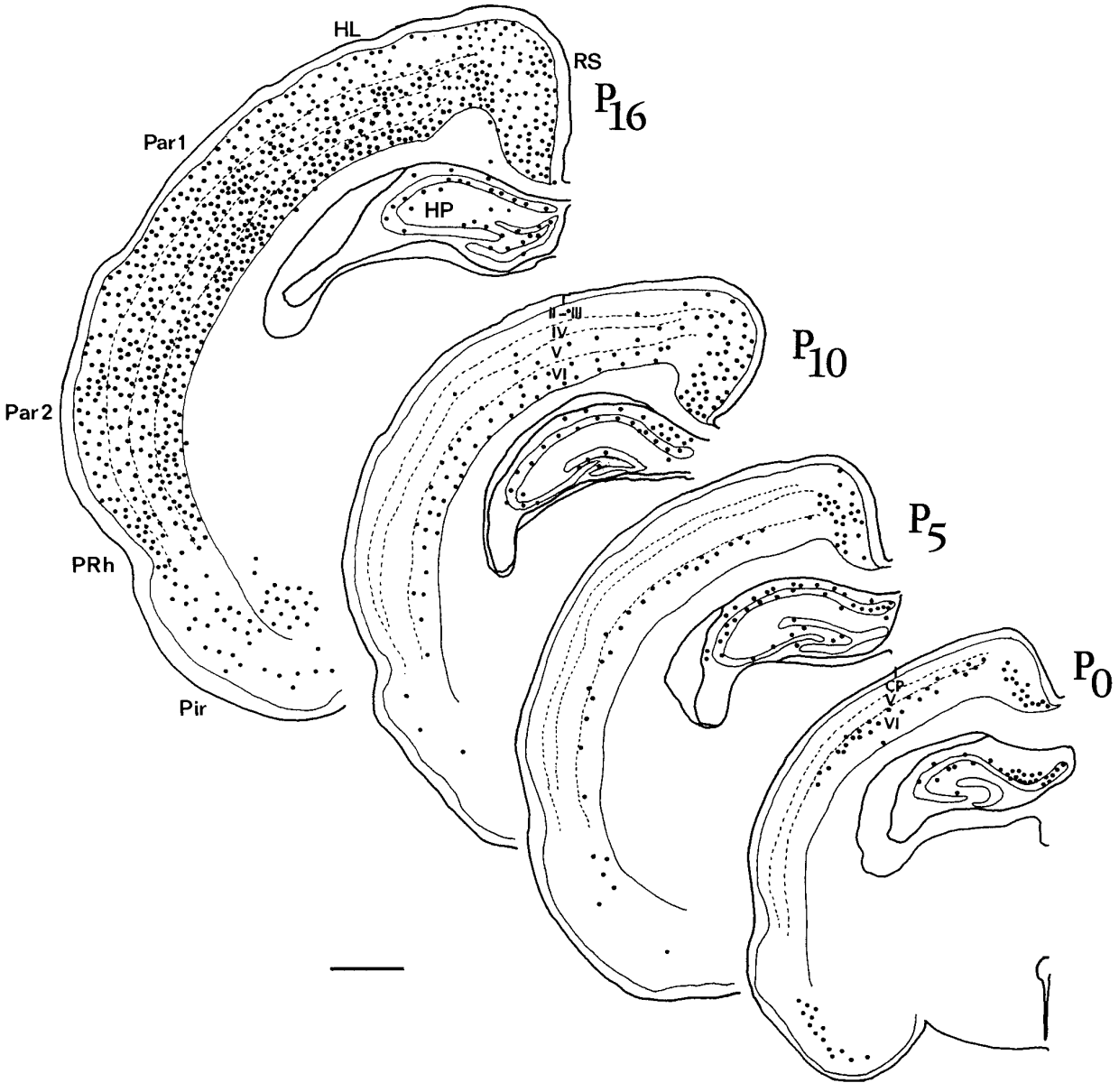

Figure 7. Camera lucida drawings showing the distribution of preprocortistatin mRNA in coronal sections of the cerebral cortex at *P0*, *P5*, *P10*, and *P16* at equivalent rostrocaudal levels. Each *dot* represents three labeled cells except in the *P0* drawing, in which each positive cell is represented by a *dot*. *CP*, Cortical plate; *HL*, hindlimb area; *HP*, hippocampus; *Par1*, parietal cortex, area 1; *Par2*, parietal cortex, area 2; *Pir*, piriform cortex; *PRh*, perirhinal cortex; *RS*, retrosplenial cortex; *I–VI*, cortical layers. Cortical areas were labeled according to Paxinos and Watson (1988). Scale bar, 1 mm.

of somatostatin itself (de Lecea et al., 1996). Thus, in some cases, cortistatin and somatostatin may be released from different terminals or they may compete for the same receptors. In addition, a previous study in adult rats showed that cysteamine-induced release of somatostatin potentiates the response of dentate granule cells to perforant path stimulation (Takazawa et al., 1994). In contrast, our electrophysiological data showed that iontophoretic administration of cortistatin had no effect on PS amplitudes in the adult dentate gyrus. These data provide indirect evidence for a putative cortistatin receptor. The lack of effect of cortistatin on PS amplitudes in the adult dentate gyrus could be attributable to a disparity in brain size and packing density of neurons in the brains of P15 and adult rats. However, the iontophoretic currents and the duration of the application of cortistatin in this study were similar to the parameters used in our previous study in which cortistatin suppressed PS amplitudes in the CA1 region of adult rats (de Lecea et al., 1996).

The cells in which most neuropeptides are produced are calbindin-positive (Hendry et al., 1984b; de Felipe, 1993). The calbindin-positive population of cortical interneurons has been considered nonoverlapping with basket and chandelier cells, which are stained with parvalbumin antibodies. However, a recent report (Alcántara et al., 1996) has determined that as many as 10% of calbindin neurons are also immunoreactive for parvalbumin in the adult rat neocortex. Thus, it is noteworthy that cortistatin is coexpressed with parvalbumin in some cortical and hippocampal interneurons. The extent of colocalization between cortistatin mRNA and parvalbumin (70%) and calbindin (47%) indicates that cortistatin mRNA is localized preferentially in neurons that are double-positive for calbindin and parvalbumin.

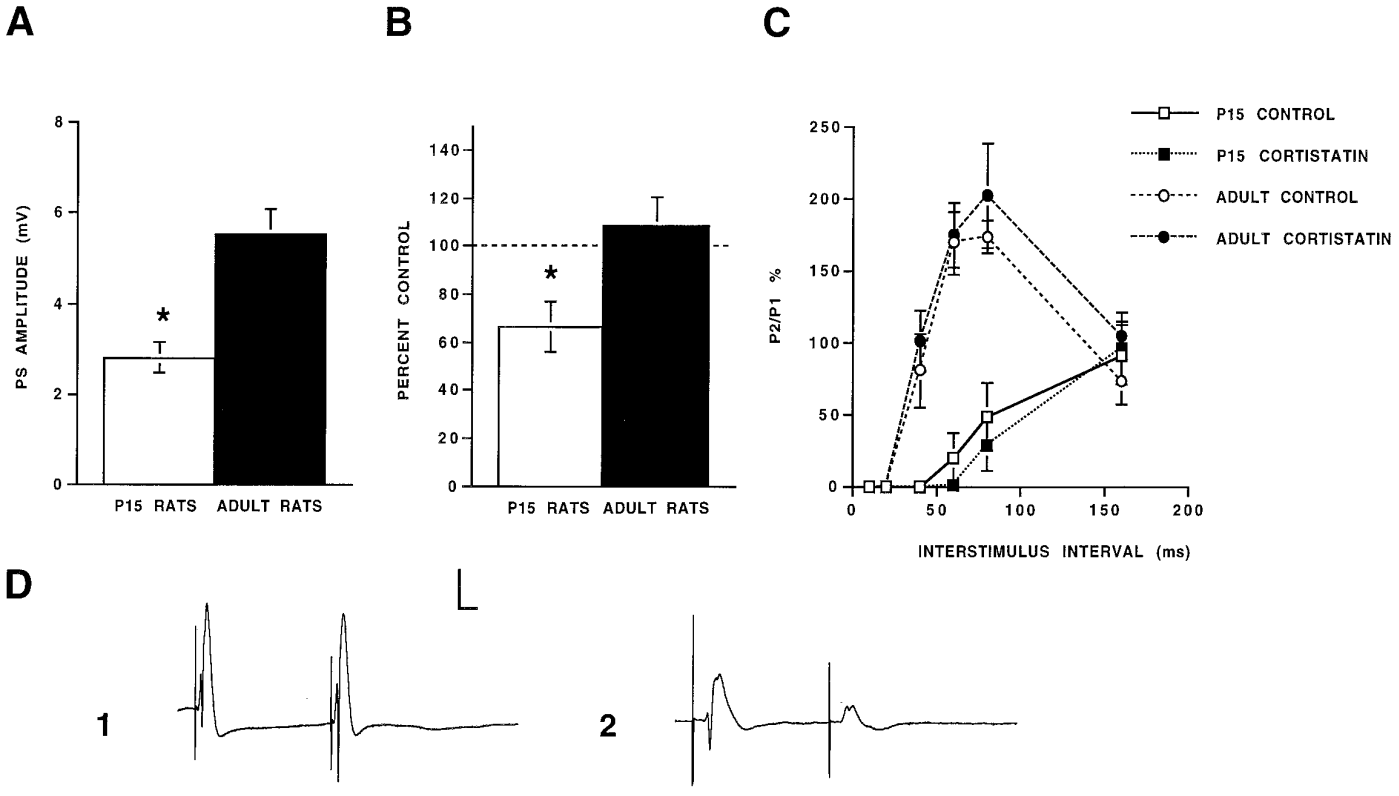

Figure 8. Electrophysiological characterization of cortistatin actions on dentate function during development. *A*, Population spike (PS) amplitudes elicited in P15 rats ($n = 7$) were significantly lower than in adult rats ($n = 6$; *asterisk* represents significance levels of $p < 0.05$; ANOVA). *B*, Iontophoretic administration of cortistatin significantly reduced PS amplitudes in P15 rats ($n = 5$; $p < 0.05$) but had no effect on PS amplitudes elicited in adult rats ($n = 6$; $p > 0.05$). *C*, Stimulation of the perforant path in P15 rats was characterized by a longer period of early inhibition. Control paired-pulse (PP) responses between P15 and adult rats were significantly different at 40, 60, and 80 msec ($n = 5$; $p < 0.05$). Administration of cortistatin had no effect on PP responses in either group ($n = 5$/group; $p > 0.05$). *D*, Representative recordings of wave forms evoked in the dentate gyrus by perforant path stimulation (50% maximum) from an adult rat (*1*) and a P15 rat (*2*). The marked facilitatory PP response at 80 msec recorded from the adult rat (*1*) contrasts with the PP response elicited in the P15 rat (*2*). Calibration: 5 mV, 10 msec.

Hippocampal neurons that contain somatostatin or parvalbumin have been well characterized in terms of their electrophysiological and anatomical properties (Lacaille et al., 1987; Sik et al., 1995; Freund and Buzsáki, 1996). The presence of preprocortistatin mRNA in a substantial portion of parvalbumin-positive fast-firing cells suggests a possible biphasic mode of action of parvalbumin interneurons: a fast mode that releases GABA and acts on $GABA_a$ receptors on pre- and postsynaptic cells and a slow mode involving cortistatin release and G-protein signaling. It is possible that cortistatin regulates principal cells at multiple levels.

In a previous report we showed that cortistatin enhanced slow wave sleep (SWS), whereas somatostatin does not have any effect on SWS but increases rapid eye movement sleep. Also, in contrast to somatostatin, cortistatin antagonizes the effects of acetylcholine on hippocampal and cortical activity (de Lecea et al., 1996). Cortical somatostatin-containing cells are known to receive input from GABAergic and cholinergic projection cells in the basal forebrain (Freund and Meskenaite, 1992) and from serotonergic neurons in the median raphe (Halasy et al., 1992). Because single interneurons contact multiple pyramidal cells and can synchronize pyramidal activity, this afferent specificity has been proposed as a mechanism for tight control of the output of principal cells (Cobb et al., 1995). Thus, it may be that cholinergic afferents innervate preferentially cortistatin-containing cells, providing a circuitry for sleep onset. Consistent with this hypothesis is the fact that a substantial proportion of cortistatin-positive cells reside in the deep layers throughout the cortex. Because most afferent axons to the thalamus originate in the deep layers of the cerebral cortex, cortistatin may be regulating the corticothalamic interactions that originate EEG spindle activity, a type of EEG wave that occurs at the onset of SWS (Steriade et al., 1993a). Also, because of its anatomical distribution and electrophysiological properties, cortistatin could be a major factor in the maintenance and synchronization of the slow oscillation (<1 Hz), a cortical rhythm that is characterized by depolarizing episodes of pyramidal and GABAergic cells and accompanies delta activity (Steriade et al., 1993b).

The developmental expression of preprocortistatin mRNA shows three major features in the cerebral cortex: (1) cortical neurons express cortistatin mRNA after the typical inside-out gradient of cortical maturation (i.e., first in deep layers and later in upper cortical layers) (Rakić, 1988); (2) preprocortistatin mRNA concentration is maximal during the second postnatal week; and (3) at P15–P21 the number of labeled neurons was higher than in the adult, indicating a transient expression at these stages and subsequent downregulation. These stages also correspond to the maturation of cortical function. It may be of significance that cortistatin mRNA is most abundant in the visual cortex and that its peak of expression occurs during the second postnatal week, coincident with eye opening. Previous studies have pointed out that the maturation of cortical interneurons is simultaneous with the first appearance of postsynaptic inhibitory

potentials and burst-firing responses linked to NMDA receptors (Luhmann and Prince, 1991). These changes in physiological responses of developing neurons may be associated with the appearance of specific NMDA receptor subunits during the second postnatal week (Williams et al., 1993). The transient expression of preprocortistatin mRNA at late postnatal stages in cortical development is similar to that reported for other neuropeptides such as somatostatin or NPY (Parnavelas and Cavanagh, 1988). Particularly interesting is the transient expression of preprocortistatin mRNA in the dentate gyrus. *In vivo* field recordings showed a high degree of intrinsic inhibition in the dentate of P15 rats. In these animals high-frequency perforant path stimulation failed to produce long-term potentiation in granule cells, in contrast with our previous reports in adult rats (Criado et al., 1996). Also in contrast to adult rats, iontophoretic application of cortistatin in the hilus of P15 rats significantly reduced the evoked PS amplitudes, suggesting that cortistatin receptors may be expressed in this area and functional at this age. However, despite this evidence for expression of preprocortistatin and a cortistatin receptor and the electrophysiological properties of dentate granule cells, in the absence of a specific cortistatin antagonist it is not possible to establish a causal relationship between the presence of preprocortistatin mRNA and the depressed state of granule cells in the second postnatal week.

Nevertheless, these considerations suggest that the developmental expression of cortistatin is a reflection of major changes in the electrical activity of a distinct subset of GABAergic cells. GABAergic stimulation has been shown to regulate the phenotype of hippocampal interneurons via the action of brain-derived neurotrophic factor (BDNF) (Marty et al., 1996). The transient increase in preprocortistatin mRNA expression during the second postnatal week could be attributable to increased BDNF activity caused by GABAergic stimulation of cortical neurons. In contrast, at later developmental stages when GABA inhibits BDNF expression (Berninger et al., 1995), cortistatin mRNA concentration is decreased. Thus, in addition to its synchronization properties described in adult animals, cortistatin may be involved in refining cortical activity, possibly modulating the establishment of synaptic connections in the neocortex and hippocampus during development.

REFERENCES

Acsády L, Halasy K, Freund TF (1993) Calretinin is present in nonpyramidal cells of the rat hippocampus. III. Their inputs from the median raphe and medial septal nuclei. Neuroscience 52:829–841.

Alcántara S, de Lecea L, del Rio JA, Ferrer I, Soriano E (1996) Transient colocalization of parvalbumin and calbindin in the postnatal cerebral cortex: evidence for a phenotypic shift in developing nonpyramidal neurons. Eur J Neurosci 8:1329–1339.

Araujo DM, Lapchak PA, Collier B, Quirion R (1990) Evidence that somatostatin enhances endogenous acetylcholine release in the rat hippocampus. J Neurochem 55:1546–1555.

Bekenstein JW, Lothman EW (1991) A comparison of the ontogeny of excitatory and inhibitory neurotransmission in the CA1 region and dentate gyrus of the rat hippocampal formation. Brain Res Dev Brain Res 63:237–243.

Berninger B, Marty S, Zafra F, da Penha Berzaghi M, Thoenen H, Lindholm D (1995) GABAergic stimulation switches from enhancing to repressing BDNF expression in rat hippocampal neurons during maturation *in vitro*. Development 121:2327–2335.

Cauli B, Audinat E, Lambolez B, Angulo MC, Ropert N, Tsuzuki K, Hestrin S, Rossier J (1997) Molecular and physiological diversity of cortical nonpyramidal cells. J Neurosci 17:3894–3906.

Celio MR (1986) Parvalbumin in most γ-aminobutyric acid-containing neurons of the rat cerebral cortex. Science 231:995–997.

Cobb SR, Buhl EH, Halasy K, Paulsen O, Somogyi P (1995) Synchronization of neuronal activity in hippocampus by individual GABAergic interneurons. Nature 378:75–78.

Criado JR, Steffensen SC, Henriksen SJ (1996) Microelectrophoretic application of SCH-23390 into the lateral septal nucleus blocks ethanol-induced suppression of LTP, *in vivo*, in the adult rodent hippocampus. Brain Res 716:192–196.

Danielson PE, Forss-Petter S, Brow MA, Calavetta L, Douglass J, Milner RJ, Sutcliffe JG (1988) p1B15: a cDNA clone of the rat mRNA encoding cyclophilin. DNA 7:261–267.

de Felipe J (1993) Neocortical neuronal diversity: chemical heterogeneity revealed by colocalization studies of classic neurotransmitters, neuropeptides, calcium-binding proteins, and cell surface molecules. Cereb Cortex 3:273–289.

de Lecea L, Soriano E, Criado JC, Steffensen SJ, Henriksen SJ, Sutcliffe JG (1994) Transcripts encoding a neural membrane CD26-like protein are stimulated by synaptic activity. Mol Brain Res 25:286–296.

de Lecea L, del Rio JA, Soriano E (1995) Developmental expression of parvalbumin mRNA in the cerebral cortex and hippocampus of rat. Mol Brain Res 32:1–13.

de Lecea L, Criado JR, Prospero O, Gautvik KM, Schweitzer P, Danielson P, Dunlop CLM, Siggins GR, Henriksen SJ, Sutcliffe JG (1996) A cortical neuropeptide with neuronal depressant and sleep-modulating properties. Nature 381:242–245.

de Lecea L, Ruiz-Lozano P, Danielson PE, Peelle-Kirley J, Foye P, Frankel WN, Sutcliffe JG (1997) Cloning, mRNA expression, and chromosomal mapping of human and mouse cortistatin. Genomics, in press.

Esclápez M, Houser CR (1995) Somatostatin neurons are a subpopulation of GABA neurons in the rat dentate gyrus: evidence from colocalization of preprosomatostatin and glutamate decarboxylase mRNAs. Neuroscience 64:339–355.

Freund TF, Buzsáki G (1996) The interneurons of the hippocampus. Hippocampus 6:347–470.

Freund TF, Meskenaite V (1992) γ-Aminobutyric acid-containing basal forebrain neurons innervate inhibitory interneurons in the neocortex. Proc Natl Acad Sci USA 89:738–742.

Gulyás AI, Freund TF (1996) Pyramidal cell dendrites are the primary targets of calbindin D28k-immunoreactive interneurons in the hippocampus. Hippocampus 6:525–534.

Halasy K, Miettinen R, Szabat E, Freund TF (1992) GABAergic interneurons are the major postsynaptic targets of median raphe afferents in the rat dentate gyrus. Eur J Neurosci 4:144–153.

Hendry SHC, Jones EG (1985) Morphology of synapses formed by cholecystokinin-immunoreactive axon terminals in regio superior of rat hippocampus. Neuroscience 16:57–68.

Hendry SHC, Jones EG, Emson PC (1984a) Morphology, distribution, and synaptic relations of somatostatin and neuropeptide Y immunoreactive neurons in rat and monkey neocortex. J Neurosci 4:2497–2517.

Hendry SHC, Jones EG, deFelipe J, Schmechel D, Brandon C, Emson PC (1984b) Neuropeptide-containing neurons in the cerebral cortex are also GABAergic. Proc Natl Acad Sci USA 81:6526–6530.

Jacobowitz DM, Winsky L (1991) Immunocytochemical localization of calretinin in the forebrain of the rat. J Comp Neurol 304:198–218.

Kawaguchi Y, Hama K (1987) Fast-spiking nonpyramidal cells in the CA3 region, dentate gyrus, and subiculum of rats. Brain Res 425:351–355.

Kondo M, Sumino R, Okado H (1997) Combinations of AMPA receptor subunit expression in individual cortical neurons correlate with expression of specific calcium-binding proteins. J Neurosci 17:1570–1581.

Kosaka T, Wu JY, Benoit R (1988) GABAergic neurons containing somatostatin-like immunoreactivity in the rat hippocampus and dentate gyrus. Exp Brain Res 71:388–398.

Lacaille JC, Mueller AL, Kunkel DD, Schwartzkroin PA (1987) Local circuit interactions between oriens/alveus interneurons and CA1 pyramidal cells in hippocampal slices: electrophysiology and morphology. J Neurosci 7:1979–1993.

Liu YB, Lio PA, Pasternak JF, Trommer BA (1996) Developmental changes in membrane properties and postsynaptic currents of granule cells in rat dentate gyrus. J Neurophysiol 76:1074–1088.

Luhmann HJ, Prince DA (1991) Postnatal maturation of the GABAergic system in the rat cortex. J Neurophysiol 65:599–615.

Mancillas JR, Siggins GR, Bloom FE (1986) Somatostatin selectively enhances acetylcholine-induced excitations in rat hippocampus and cortex. Proc Natl Acad Sci USA 83:7518–7521.

Marty S, Berninger B, Carroll P, Thoenen H (1996) GABAergic stimu-

lation regulates the phenotype of hippocampal interneurons through the regulation of brain-derived neurotrophic factor. Neuron 16:565–570.
Miettinen R, Gulyás AI, Baimbridge KG, Jacobowitz DM, Freund TF (1992) Calretinin is present in nonpyramidal cells of the rat hippocampus. II. Coexistence with other calcium-binding proteins and GABA. Neuroscience 48:29–43.
Morrison JH, Benoit R, Magistretti PJ, Bloom FE (1983) Immmunohistochemical distribution of prosomatostatin-related peptides in cerebral cortex. Brain Res 262:344–351.
Morrison JH, Magistretti PJ, Benoit R, Bloom FE (1984) The distribution and morphological characteristics of the intracortical VIP cell: an immunohistochemical analysis. Brain Res 292:269–282.
Parnavelas JG, Cavanagh ME (1988) Transient expression of neurotransmitters in the developing neocortex. Trends Neurosci 11:92–93.
Paxinos G, Watson C (1988) The rat brain in stereotaxic coordinates. San Diego: Academic.
Rakić P (1988) Specification of cerebral cortical areas. Science 241:170–176.
Schibler K, Tosi M, Pittet AC, Fabiani L, Wellauer PK (1980) Tissue-specific expression of mouse α-amylase genes. J Mol Biol 142:93–116.
Schmechel DE, Vickrey BG, Fitzpatrick D, Elde RP (1984) GABAergic neurons of the mammalian cerebral cortex: widespread subclass defined by somatostatin content. Neurosci Lett 47:227–232.
Sik A, Penttonen M, Ylinen A, Buzsáki G (1995) Hippocampal CA1 interneurons: an *in vivo* intracellular labeling study. J Neurosci 15:6651–6665.
Somogyi P, Hodgson AJ, Smith AD, Nunzi MG, Gorio A, Wu J-Y (1984) Different populations of GABAergic neurons in the visual cortex and hippocampus of cat contain somatostatin- or cholecystokinin-immunoreactive material. J Neurosci 10:2590–2603.
Steriade M, McCormick DA, Sejnowski TJ (1993a) Thalamocortical oscillations in the sleeping and aroused brain. Science 262:679–685.
Steriade M, Nuñez A, Amzica F (1993b) A novel slow (<1 Hz) oscillation of neocortical neurons *in vivo*: depolarizing and hyperpolarizing components. J Neurosci 13:3252–3265.
Takazawa A, Abraham WC, Sekino Y (1994) Cysteamine potentiates entorhinal activation of dentate gyrus granule cells in rats. Brain Res Bull 33:437–443.
Veber DF, Holly FW, Nutt RF, Bergstrand SJ, Brady SF, Hirschmann R, Glitzer MS, Saperstein R (1979) Highly active cyclic and bicyclic somatostatin analogues of reduced ring size. Nature 280:512–514.
Williams K, Russel SL, Shen YM, Molinoff PB (1993) Developmental switch in the expression of NMDA receptors occurs *in vivo* and *in vitro*. Neuron 10:267–278.
Wilson DA (1984) A comparison of the postnatal development of postactivation potentiation in the neocortex and dentate gyrus of the rat. Dev Brain Res 16:61–68.
Zilles K (1985) The cortex of the rat. Berlin: Springer.